Applied Physics A (2022) 128:424
https://doi.org/10.1007/s00339-022-05568-z

Applied Physics A
Materials Science & Processing

Synthesis of sericin coated silver nanoparticles (Ag-Ser) by modified Tollens' method and evaluation of colloidal stability

Mert Saraçoğlu[1,2] · Merve B. Bacınoğlu[3] · Sıddıka Mertdinç[1] · Servet Timur[1]

Received: 10 December 2021 / Accepted: 5 April 2022 / Published online: 22 April 2022

Abstract

In this study, sericin extracted from *Bombyx mori* silk cocoons was integrated into the well-known Tollens' method for synthesizing Ag-NPs. Sericin successfully acted as a stabilizer while silver amine complex $[Ag(NH_3)_2]^+$ was reduced by maltose. As a result, silver nanoparticles with high stability are formed. Possible functional groups related to the stabilization of NPs were investigated by Fourier-transforms infrared spectroscopy (FT-IR). Ag-Ser NPs were characterized using particle size measurements based on dynamic light scattering (DLS) and transmission electron microscopy (TEM). According to the characterization investigations, Ag-Ser NPs have characteristic (111) face-centered cubic (FFC) plane and were spherical in shape with a narrow size distribution of 20.23 ± 6.25 nm. Overall, the sericin-modified Tollens' method for synthesizing Ag-NPs offers a simple and non-toxic production method to form nanoparticles. Colloidal stability of nanoparticles displays an essential role since their enhanced nano-properties can be diminished by an increase in size due to aggregation and agglomeration. Therefore, the effect of pH and electrolyte concentration on particle stability was investigated through the surface charge of Ag-Ser NPs using a Zeta-potential analyzer and change in absorption spectra by UV–Vis Spectroscopy. Results obtained from this study propose a potential synthesis route for Ag NP synthesis and may extend the applicability of silver nanoparticles in biotechnological researches as aseptic and therapeutic usages.

Keywords Silver nanoparticles · Surface functionalization · Sericin · Tollens · Method · Characterization · Colloidal stability · Agglomeration

Abbreviations

Ag-Ser NPs	Sericin stabilized silver nanoparticles
FT-IR spectroscopy	Fourier-transforms infrared spectroscopy
DLS	Dynamic light scattering
TEM	Transmission electron microscope
HRTEM	High-resolution transmission electron microscope image
SAED	Selected area (electron) diffraction

1 Introduction

Materials with at least one dimension in nanometer scale such as; nanofibers, nanocapsules, nanorods, nanotubes, and nanostructured surfaces are considered as nano-materials thus, synthesizing and controlling the nanometer scale materials are the main interest of nanotechnology [1, 2]. Nanomaterials other than their bulk forms, show superior mechanical, electrical, chemical, optical, magnetic,

✉ Mert Saraçoğlu
saracoglum16@itu.edu.tr

Merve B. Bacınoğlu
mervebegum.bacinoglu@studenti.unimi.it

Sıddıka Mertdinç
mertdinc@itu.edu.tr

Servet Timur
timur@itu.edu.tr

[1] Department of Metallurgical and Materials Engineering, Istanbul Technical University, 34467 Maslak, Istanbul, Turkey

[2] Nanosilver Co. Teknopark İstanbul, 34906 Pendik, Istanbul, Turkey

[3] Department of Medical and Biotechnology and Translational Medicine, University of Milan, Via Vanvitelli 32, 20133 Milan, Italy

thermal, or biological properties due to their high surface area [3, 4]. Among them, silver based nanoparticles are considered as the most researched nanomaterial due to their broad biocidal effect [5]. Dissolution of Ag^0 to Ag^{1+} leads to random formation of silver complexes hence inhibiting the responsible proteins for RNA–DNA replication and increase the permeability of the membrane [6]. Consequently, silver nanoparticles shows outstanding antifungal, antibacterial and antiviral properties [7]. Therefore, silver nanoparticles are extensively used in various biomedical applications including drug-delivery, wound dressings and disinfectants [7–9].

Chemical reduction of silver ions is the most commonly used nanoparticle production method due to its simplicity and being cheaper than the physical and mechanical production techniques [10]. However, using reductants and stabilizers in reduction protocols can be highly toxic for both environment and health. These chemicals hinder Ag NPs further usage in biomedical applications. To avoid such complications, green synthesis of nanoparticles is required [3].

Furthermore, the usage of silver NPs is also limited due to their instability against aggregation, where antimicrobial and catalytic activities are diminished by the aggregates that reduce the surface area of particles [11]. To benefit from enhanced properties of silver NPs, particles required to be stabilized. Stabilization occurs mainly by two mechanisms: electrostatic repulsion by charged molecules and steric repulsion by adsorption of complex polymers on the particle surface [10]. For this reason, complex biopolymers with ability to stabilize in both mechanisms, shows an excellent opportunity for green, large-scale silver nanoparticle production. In literature, natural polymers such as polysaccharides, chitosan, and gelatin have proven to stabilize nanoparticles and natural reductants, such as ascorbic acid and sugars, successfully reduce silver ion [12–16].

Sericin is also a bio-complex polymer that constitutes 20–30% of silk cocoon and preserves structure unity [17]. Over the years, the interest in sericin protein in bio-nanotechnology has been increased due to its biomedical applications because of its unique properties such as UV-protection, anti-oxidative ability and bio-compatibility [11, 18]. Sericin is selected as a stabilizing agent due to its electrostatic and steric protection thus aggregation and degradation of particles can be prevented [11].

In this study, sericin extracted from silk cocoons was used to synthesize sericin-coated silver nanoparticles (Ag-Ser NPs) based on the Tollens' process. Traditional Tollens' process was used for mirror making by depositing silver particles on a glass surface [19]. Formerly, colloidal silver nanoparticles were successfully synthesized by the Tollens' process based on pH, concentration of reaction components, and stabilizer media [20]. Additionally, particle stability was measured according to biologically relevant conditions (such as pH and %NaCl) to enable integration of NPs in biomedical uses.

This study presents the incorporation of natural ingredients in industrially adaptable Tollens' method and determination of Ag-Ser NPs' stability limits. We believe information gathered in this article could define the adaptability of Ag-NPs in biomedical applications.

2 Experimental section

2.1 Materials

Bombyx Mori silk cocoons were obtained from Kozabirlik (Bursa, Turkey) as a sericin source. Silver nitrate ($AgNO_3$, Merck™, 99.99%), ammonium hydroxide (NH_4OH, Merck™, 25% w/w), sodium hydroxide (NaOH, Merck™), D-(+)-maltose monohydrate (Merck™) were used as initial materials. Bovine Serum Albumin (BSA, Sigma-Aldrich™) and Bradford reagent (Bio Basic™) were used in experiments as raw materials. Hydrochloric acid (HCl, Merck™, 37% w/w) was used to adjust pH. Distilled water was used in all steps of the experimental procedures. All glassware equipment was immersed in 30% nitric acid (v/v) and rinsed with deionized water prior to use.

2.2 Sericin extraction

Initially, *Bombyx Mori* silk cocoons were cut into smaller pieces. Then, freshly sheared 4.5 g cocoon into 300 mL distilled water was autoclaved under the 1 atm pressure at 121 °C for 1 h. After that, Sericin solution was vacuum filtered through 2 µm filtering paper to remove any impurities [21].

2.3 Protein quantification analysis by Bradford Assay

1 mL of BSA solutions were prepared in various concentrations of 0.0, 0.125, 0.25, 0.5, 0.75, 1.0 and 1.25 (mg/mL). Each cuvette contained 1200 µL of Bradford Reagent and 20 µL of the protein samples. 3 cuvettes for each concentration were measured and the mean absorbance values were taken. Every cuvette was incubated 5 min before measuring absorbance at 595 nm. After quantifying all of the BSA solutions, the isolated sericin samples were measured in unit of mg/mL.

2.4 Synthesis of silver nanoparticles via modified Tollens method

For synthesis, the modified Tollens method was employed by addition of sericin as a stabilizer [10]. Initially, $AgNO_3$

solution was mixed with necessary amount of NaOH (based on the pH) to obtain Ag_2O. Then, stoichiometric amount of NH_4OH was titrated to the mixture to obtain silver amine complex ($[Ag(NH_3)_2]^+$). Extracted sericin solutions were added into the mixture containing silver amine complex, with concentration ranging from 10 to 25 µg/mL. Finally, maltose monohydrate solution was added to the mixture as a reducing agent. Final concentrations of reactants were: 1mM $AgNO_3$, (pH 11.5–11.8–12) NaOH, stoichiometric amount of $NH_{3(aq)}$ (10–15–20–25 µg/mL) sericin and 10 mM maltose in 200 mL solution Reaction components were added to the mixture in the mentioned order with vigorous stirring. Ag-Ser NPs were stored at + 4 °C under light-sensitive conditions to avoid further agglomeration of particles.

2.5 ATR-FTIR spectroscopy analysis.

FTIR spectra of the specimens were recorded at room temperature in the mid-IR range (400–4000 cm^{-1}) on a Bruker Alpha-p FTIR spectrometer equipped with a Bruker Platinum ATR accessory. Sample measurements were conducted on dry, lyophilized sericin powder. Each spectrum was taken over 12 scans with a resolution of 1 cm^{-1}. Obtained results were analyzed using OPUS Software (Bruker Optics). For all experiments, Ag-Ser NPs synthesized with 1 mM $AgNO_3$ and 25 µg/mL sericin at pH of 11.5 were used.

2.6 Nanoparticle characterization

The mean particle size of Ag-Ser NPs was recorded using particle size analyzer NanoFlex™ particle measurement device, based on the dynamic light scattering (DLS). All experiments were repeated three times prior to measurement. JEOL JEM 2100 transmission electron microscope (TEM) operating at 200 kV, was used for morphological analysis of the synthesized Ag-Ser nanoparticles. Nanoparticle diameters were calculated using ImageJ processing and analysis software (version v1.52a) by measuring 100 diameters of the particle from 3 different TEM images at 15.000× magnification. Additionally, selected area diffraction patterns (SADP) were taken from TEM images to help the phase identification of the silver nanoparticles.

2.7 UV–Vis spectroscopy analysis

For investigate the stability of the NPs, the pH of NP samples was adjusted either by NaOH or HCl. Ag NP samples were mixed with different NaCl concentrations to prepare NaCl-NP suspensions ranging from 0 to 3% and 4 to 12% w/w. UV–Vis spectrums of pH and salt suspensions were recorded between 380 and 550 nm on BIO-RAD, BenchMark™ Plus microplate reader, for 3 cycles with a resolution of 2 nm^{-1}. All suspensions were left standing overnight in dark at 25 °C before measurements.

2.8 Zeta-potential measurements

Zeta potential of nanoparticle solutions was measured using Litesizer™ 500 apparatus (Anton Paar). The zeta-potential cuvette has a Ω-shaped capillary tube with an applied potential of 200 V at 25 °C. pH suspensions were prepared either by NaOH or HCL and shaken for 30 min before measurement.

3 Results and discussion

3.1 Extraction and analysis of sericin protein

Sericin was extracted from silk cocoons for further usage in Ag-Ser NP synthesis. Sericin protein can be extracted by heat, acids, and bases. The biological and physical properties of sericin can be affected by different extraction methods [21]. In this work, sericin has extracted by autoclaving for 60 min at 0.1 MPa with a degumming rate of 18–25% of total cocoon mass. This process is selected among others due to its simplicity and not contain any further purification steps [22].

Sericin molecules show characteristic amide (I-II-III) peaks in the IR spectrum. Amide I peak generally corresponds 1630–1650 cm^{-1} due to C=O stretching vibration whereas, N–H bending and C–N stretching vibration at 1520–1540 cm^{-1} for amide II and C–N stretching vibration together with N–H in-plane bending at 1270–1230 cm^{-1} for amide III [17, 23]. From FTIR measurements (Fig. 1)

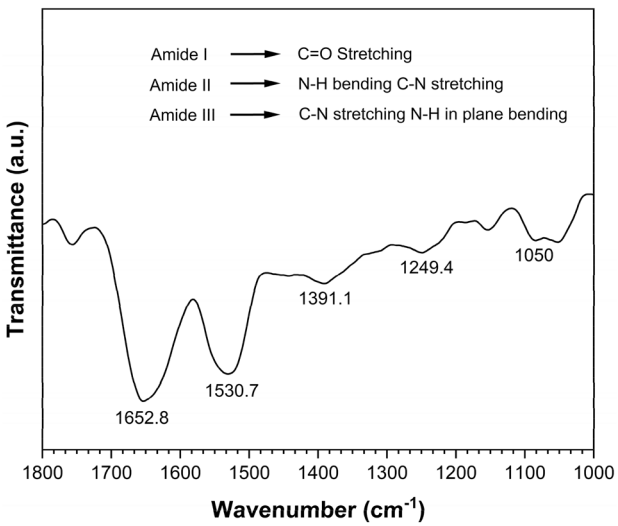

Fig. 1 FTIR spectra of freeze dried sericin powder

amide (I–II–III) peaks were detected at 1652.8, 1530.7, and 1249.4 cm^{-1}, respectively. It is worth to mention that the amide I and amide II presents the major peaks in the spectra corresponding to C=O stretching. Thus, relative intensity of C=O peaks indicates extracted sericin structure abundantly contains highly hydrophilic carboxylate groups [17]. Moreover, absorptions at 1050 and 1391 cm^{-1} arise from C–H and O–H bending vibration and C–OH stretching vibration also indicates structure rich in hydroxyl chains [23].

Furthermore, amide bonds are the backbone of polypeptide chains thus, their absorptions in IR spectra could indicate molecular conformations and secondary structures of the proteins [23]. In a previous study, random coil structures were assigned to 1650 cm^{-1} for amide I, 1540 cm^{-1} for amide II and 1230 cm^{-1} for amide III [17]. As mentioned before, peaks that found at 1652.8, 1530.7 and 1249.4 cm^{-1} may show, sericin protein consist of a high degree of random coils [24]. This molecular conformation may suggest that the sericin molecules have denatured and degraded due to high temperature-high pressure extraction method. Thus, abundance of highly electronegative functional groups appeared on IR spectra, may produce an electrostatic barrier while, complex polymer structure provides a physical barrier to particle aggregation. Therefore, denatured sericin may be a promising stabilizing agent for nanoparticle synthesis.

3.2 (Ag-Ser) nanoparticle preparation and evaluation of synthesis parameters

Silver nanoparticle synthesis by Tollens process involves three reactions; formation of silver oxide by dissolution of $AgNO_3$ in presence of NaOH (Eq. 1), alteration of silver oxide to silver amine complex (Eq. 2) and reduction of silver amine complex cation in alkaline media by a reducing sugar (Eq. 3).

$$2AgNO_3 + 2NaOH \rightarrow Ag_2O_{(s)} + 2NaNO_3 + H_2O \quad (1)$$

$$Ag_2O_{(s)} + 4NH_3 + H_2O \rightarrow 2\left[Ag\left(NH_3\right)_2\right]OH \quad (2)$$

$$R - CHO + 2\left[Ag\left(NH_3\right)_2\right]OH \rightarrow 2Ag_{(s)} + 4NH_3 + H_2O + R - COOH \quad (3)$$

In nanoparticle synthesis, size distribution, morphology and stability are dependent on concentration of reaction components, type of reducing and stabilizing agents [25]. During the reduction of silver complex, ammonium concentration was remained same in all experiments since, excess NH_3 ions in solution surround the amine complexes where, fewer silver nuclei can be formed due to slower reaction kinetics. Consequently, the particle size prone to be larger [26].

In addition to ammonium concentration, pH value of the solution is also a crucial parameter for the Tollens process. As the pH of the reaction environment increased above 12, thick silver layer forms on the glass surface. (see Supp. data) Consequently, particle production yield decreases. This phenomenon was also reported by S. Sangsuk [27]. In their work, sonication was applied in reaction system to avoid mirror formation. On the other hand, at pH values lower than 11.5 prolong reaction time from minutes to hours. Therefore, optimum pH values were determined between 11.5 and 12.

Particle size measurement results (Table 1) show that size distribution of Ag-Ser NPs was increased from 20.23 ± 6.25 to 51.8 ± 23.01 nm from pH 11.5 to pH 12. Results are consistent with previous studies, in which at pH of 11.5, both mean particle size and distribution become narrower [26]. Remarkably, adjusting pH of synthesis media to 11.5, provide both smaller average particle size and narrower standard deviation.

As for the sericin concentration (Table 2), the lowest particle size value (18.04 ± 6.03) were enabled via 25 µg/mL sericin concentration. Results suggest that reaction time can be affected by stabilizer concentration together with pH of the solution. Moreover, controlling both parameters has a crucial role in synthesizing nanoparticles with optimum anti-bacterial activity since silver nanoparticles' anti-bacterial efficiency depends on their size [28].

3.3 TEM results and estimation of sericin coating on Ag-Ser NPs

According to our TEM results (Fig. 2A,B), Ag-Ser NPs were consisted spherical particles with no indication of aggregation and each equiaxed spherical shaped particles have relatively same length. Additionally, on a single nanoparticle (Fig. 2B) orientation of different crystal planes are observed. Particle size histogram (Fig. 2D) of synthesized nanoparticles present a relatively narrow distribution compared to other green synthesis methods and stabilizers [29, 30]. HRTEM image (Fig. 2C) presents Ag-Ser NPs have periodic lattice spacing of 0.23 nm, which consistent

Table 1 Average particle sizes of synthesized Ag-Ser NPs at different pH conditions measured by Dynamic Light Scattering (DLS)

pH[a]	11.5	11.8	12
Average particle size[b] (nm)	20.23 ± 6.25	38.7 ± 14.5	51.8 ± 23.01

[a] pH of solutions was measured before addition of maltose solution

[b]Concentration of sericin was kept same in all pH experiments (20 µg/mL)

Table 2 Average particle sizes of Ag-Ser NPs at different sericin concentrations measured by dynamic light scattering (DLS)

Sericin conc. (µg/mL)	10	15	20	25
Average particle size[a] (nm)	30.86 ± 7.8	28.9 ± 7.41	20.23 ± 6.25	18.04 ± 6.03

[a]pH of the solution were kept at 11.5 for all experiments

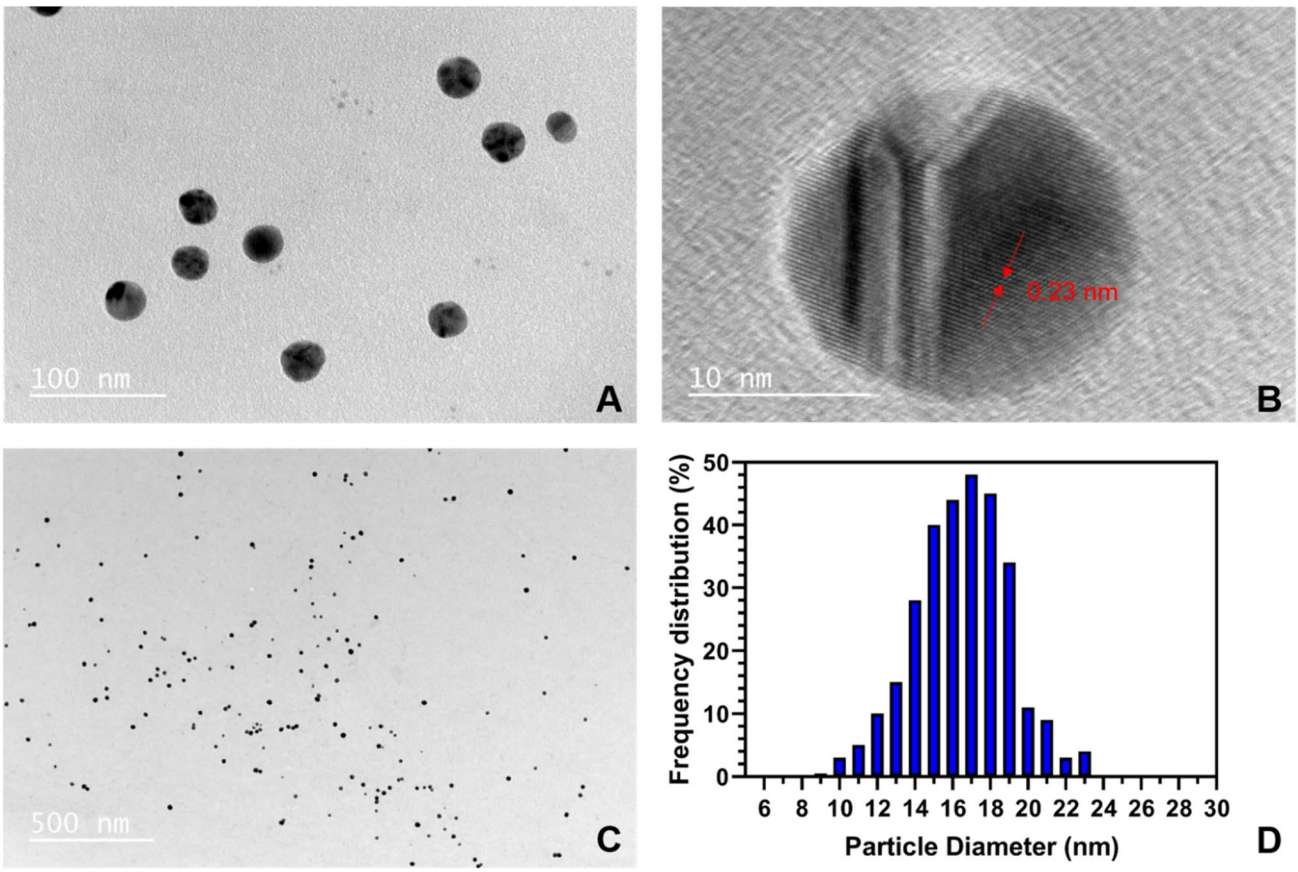

Fig. 2 **A** TEM image of synthesized Ag-Ser NPs synthesized at pH 11.5, with 25 µg/mL sericin concentration (×40,000). **B** corresponding HRTEM image of single nanoparticle (× 500,000). **C** At 500 nm range (×15,000). **D** Corresponding particle size distribution of Fig. 3C (16.03 ± 2.3 nm)

with the characteristic plane of (111) for face-centered cubic (FCC) structure [31, 32].

SAED patterns (Fig. 3A,B) present a ring and spot diffraction pattern which also indicates polycrystalline nature of Ag-Ser NPs [33]. However, we detected some highly crystalline particles which further prove the ripening of particles at the growth stage. Interplanar distances ($d_{calculated}$) of patterns were found to be 2.33, 1.95, 1.37, 1.08, 0.85 and 1.04 Å which corresponds to (111), (200), (220), (222), (422) and (400) planes of face centered cubic structure (FCC) which is specific for Ag crystal structure [34, 35].

To investigate that the extracted sericin can encapsulate synthesized particles and stabilize the growth stage, TEM analyses were used. Transmission electron spectroscopy only provides particle images without the organic component due to the proteins' electron transparency [4]. Apart from the previous TEM images, Ag-Ser NPs synthesized at 50 µg/mL (Fig. 4) clearly shows that the presence of polymer which became visible with increasing sericin concentration. This phenomena was also seen in the collagen coated gold NPs where collagen seen as transparent of the TEM image [36].

3.4 Stability measurements of (Ag-Ser) nanoparticles for biological platforms

UV–Vis spectroscopy provides significant information to determine particle properties by the collective electron oscillations, known as surface plasmons, can be excited by the

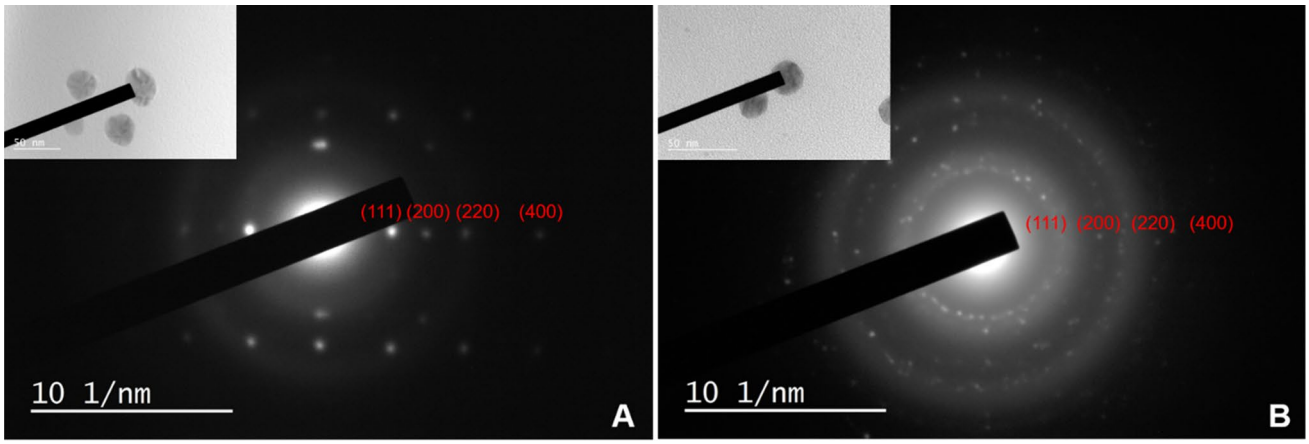

Fig. 3 SAED patterns of Ag-Ser NPs synthesized at pH 11.5, with 25 µg/mL sericin concentration. Patterns obtained from different particles showing crystallization degree of each individual particle (**A**, **B**). The inset of each pattern presents the respective pattern region

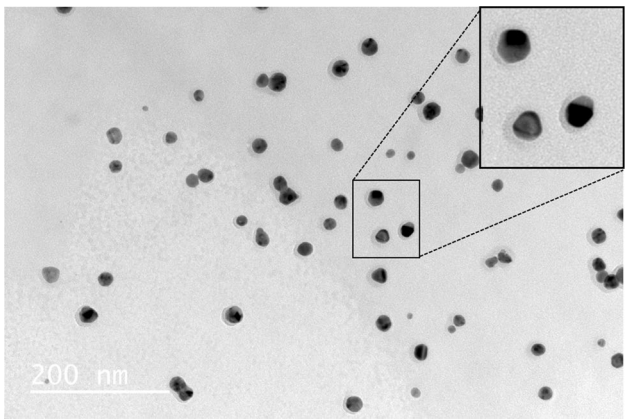

Fig. 4 TEM image of Ag-Ser NPs synthesized at pH 11.5, with 50 µg/mL sericin concentration in 200 nm range, the inset shows the encapsulated nanoparticles

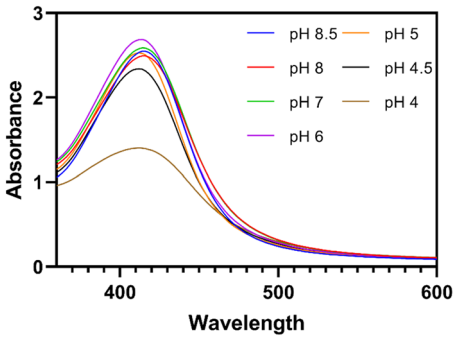

Fig. 5 **A** UV–Vis absorption spectrums of Ag-Ser NPs at different pH values and **B** enlargement of absorption spectrum at λ_{max} for pH values between 8 and 4 (Ag-Ser NPs synthesized at pH 11.5, 25 µg/mL sericin concentration)

incoming light. The oscillation frequency is strongly affected by the media's dielectric properties and the metal, particle size, and shape. Therefore, this technique displays distinctive absorption features in the spectrum according to change in particle properties [37, 38]. During the synthesis, the colorless solution was changed to yellow then brownish-yellow. The color change indicates the formation of silver NPs. This phenomenon arises from absorption of wavelengths between 380 and 450 by the silver NPs due to surface plasmon resonance [12].

The stability of particles is strongly affected by surrounding environmental conditions such as pH and ionic strength [39]. Therefore, preserving the stability between the particles in different situations have crucial importance for the applicability of silver nanoparticles in biological systems where bio-availability, mobility, and anti-biocidal activity can be altered by aggregation of particles [40].

To evaluate the effect of pH on the stability of Ag-Ser NPs, the absorption spectra were analyzed for the detection of possible destabilization at biologically relevant pHs, from 8.5 to 4. In spectrums, absorbance at full maxima was significantly reduced at pH of 4.5 (Fig. 5). In literature, agglomeration mainly attributed by the occurrence of a second peak at the band between 500 and 600 nm [41]. Therefore, decrease in absorbance may be the consequence of either dissolution or precipitation.

To further investigate the behavior of nanoparticles at different pHs, Zeta-potential of Ag-Ser NPs were measured. Zeta potential is a quantitative parameter, which shows the charge difference between the nanoparticle surface and the surrounding medium [4]. At high ζ-values, the surface charge of particles is strong enough to overcome attraction forces (in this case, Van der Waals forces) [42]. Therefore,

evaluating the surface potential could be a useful tool to understand the electrostatic stability of Ag-Ser NPs.

When synthesized nanoparticles have considerable positive or negative ζ-value (> ± 30 mV), repulsion forces between particles are supposed to be high. Thus, particles will not intent to be agglomerated [43]. In the nanoparticle–sericin system, charge difference emerges from negative -oxo, -hydroxo, sulfide, and carbonyl groups from sericin coating and free OH^- ions in the solution environment [42].

At the start, synthesized particles have a **ζ-**value of − 29.8 mV at a pH of 10 (Table 3). Besides, at a pH of 7, ζ-value was − 27.7 mV. Such a high potential value at a pH of 7 indicates that the sericin alone can provide a negative charged electrostatic barrier to nanoparticles. Although no significant change was observed at alkaline conditions, ζ-values were decreased at acidic pHs, from − 27.7 to − 15.3 mV, approached zero. This hypothesis agrees with the isoelectronic point of sericin (3.6–4), where the protein's net charge becomes zero at pH of 7 [44].

Agglomeration is a reversible process, which can be defined as the formation of bigger precipitates by weak physical interactions [45]. In this case, agglomeration occurs rather than aggregation because sericin coating acts as a physical barrier even though the protective potential layer was decreased. Therefore, in alkaline pH values, when enough concentration of hydroxyl ion is present in the solution, particles can re-disperse (Fig. 6). These phenomena also could be seen when a complex polymer with electronegativity such as casein [46] is used in nanoparticle synthesis. Based on our experiments, it can be concluded that the agglomeration and later precipitation of NP agglomerates is the main reason of decrease in absorption in pH spectrums (Fig. 6). Thus, pH 4.5 (ζ value = − 15.3) is determined as a critical limit for the overwhelming electrostatic forces between particles by attraction forces.

As for the comparison, synthesized NPs have higher surface potential than citrate stabilized nanoparticles (− 21.17 mV at pH 7) [47]. Besides, sodium dodecyl sulfate [48] (SDS) and cetyltrimethylammonium bromide [49] (CTAB) coated NPs have the zeta potential of − 40 mV and + 34 mV, respectively. However, their active stabilization mechanism is only limited by electrostatic repulsion forces due to their amphiphilic structure. Results demonstrate that the Ag-Ser NPs have electrostatic stability between pH range of 5 and 9 with having ζ-value of − 27.7 mV at pH 7. Furthermore, Ag-Ser NPs

Table 3 Zeta potential values of Ag-Ser NPs at different pHs varied from 4.5 to 10 (Ag-Ser NPs synthesized at pH 11.5, 25 µg/mL sericin concentration)

pH	4.5	5	6	7	8	9	10
ζ values (mV)	− 15.3	− 21.3	− 24.5	− 27.7	− 26.9	− 28	− 29.8
Σ	± 0.3	± 0.2	± 1	± 0.5	± 0.3	± 0.8	± 1.5

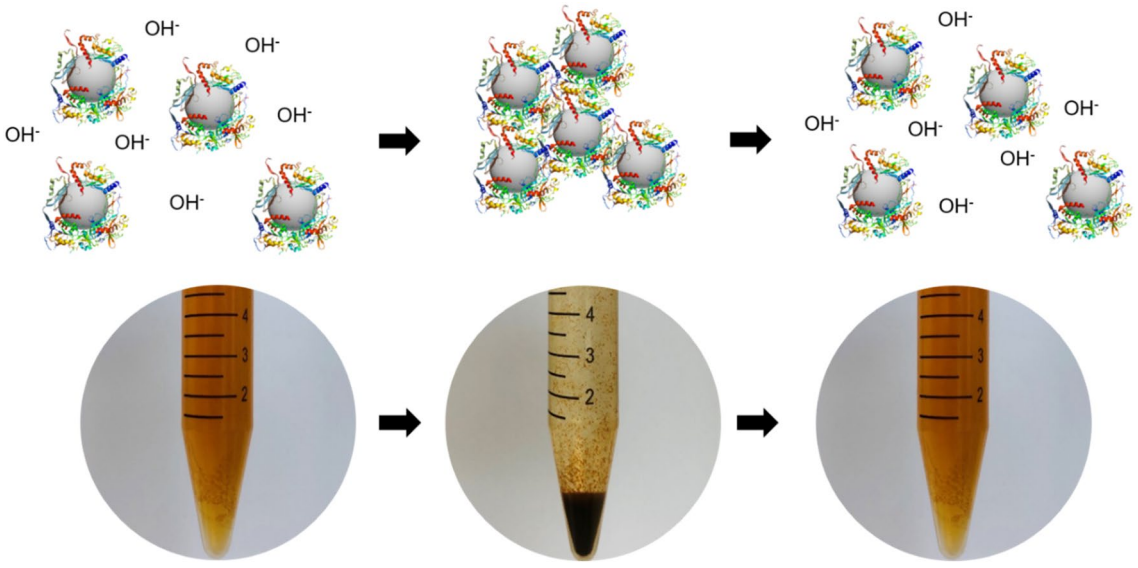

Fig. 6 A schematic illustration showing previously agglomerated Ag-Ser NPs at acidic pHs can electrostatically re-stabilize due to protection of steric forces

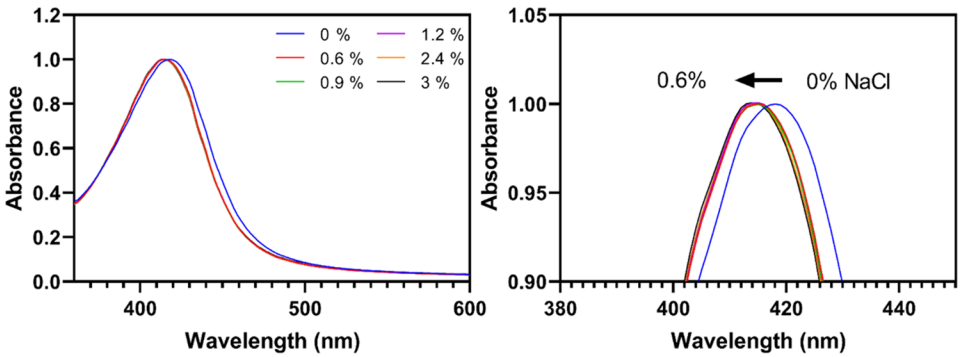

Fig. 7 **A** Normalized absorption spectrum of Ag-Ser NPs at NaCl concentrations varied from 0 to 3% after 24 h and **B** representation of absorption spectrum at λ_{max} (400 nm–430 nm) an initial blue shift was detected at NaCl concentrations between 0 and 0.6% (Ag-Ser NPs synthesized at pH 11.5, 25 µg/mL sericin concentration)

are sterically protected since particles are agglomerated at a pH of 4.5 rather than aggregated.

3.5 Effect of NaCl concentration on colloidal stability of Ag-Ser NPs

The stability of Ag-Ser NPs was assessed by mimicking the isotonic conditions at the addition of different NaCl concentrations. The absorbance of NP solutions with NaCl concentrations varying between 0 and 15% was measured. At concentrations between 0 and 3% NaCl (Fig. 7), Ag-Ser NPs show excellent stability with an initial blue shift from 418 to 414 nm at 6% NaCl were observed.

Initial blue shifting by the addition of NaCl solution was explained by Li et al. [50]. In oxygenated conditions nanoparticle surface oxidizes hence, a Ag_2O surface forms. Later, the oxidized silver surface dissolves and releases silver ions. In electrolyte free NP suspensions, adsorption of Ag^+ ions on nanoparticle surface hinders the dissolution of the Ag_2O surface. In our case, the initial addition of NaCl (0.6%) quickly breaks the Ag^+ adsorption layer by the formation of AgCl. Thus, particles start to dissolve until the Ag^+ layer reforms. However, no change was observed between concentrations of 0.6 to 4% NaCl.

At higher NaCl concentrations (Fig. 8), the Ag-Ser NP spectrum 500–600 nm were extended, suggesting the formation of aggregates [51], while the spectrum continued to blue shifting. In the light of these facts, our results indicate that when the salt concentration in solution is high enough, Cl^- ions with dissolved Ag^+ ions precipitate as AgCl between particles and promote the bridges that produce hard aggregates [42]. In short, a constant blue shifting occurs by the addition of NaCl can be explained by a decrease in the size of NPs, which nanoparticles start to dissolve in the presence of Cl^- ions. Moreover, based on our experiments, an NaCl concentration of 7% is critical for the aggregation of Ag-Ser NPs.

4 Conclusions

In this work, sericin was successfully integrated into Ag nanoparticle synthesis, and production parameters were optimized. Due to complex structure and high percentage of hydrophilic groups, sericin molecule provided both electrostatic and steric barrier for nanoparticles. Synthesized Ag-Ser NPs have average particle size distribution of 20.23 ± 6.25 nm at pH 11.5, 20 µg/mL sericin concentration. TEM results indicate that formed particles have spherical morphology and show characteristic (111) face-centered cubic (FCC) plane of silver. Colloidal stability of Ag-Ser NPs did not alter at pH range between 4.5 and 10 and 7% NaCl concentration. In contrast, synthesized nanoparticles were agglomerated when pH of the solution decreased to

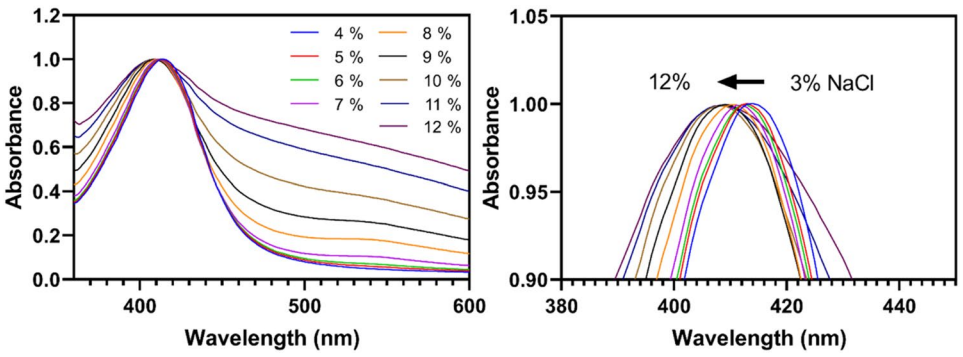

Fig. 8 Normalized absorption spectrums of **A** Ag-Ser NPs at different NaCl amounts from 4 to 12% after 24 h and **B** enlargement of absorption spectrum at λ_{max} showing the constant blue shifting accompanied increase in absorbance at wavelengths between 450 and 600 nm (Ag-Ser NPs synthesized at pH 11.5, 25 µg/mL sericin concentration)

4.5, which can be restored to previous state by increasing pH to higher values indicate that the steric stabilization between particles continue to act even though electrostatic stabilization was decreased. From the results it can be concluded that the stable Ag-Ser NPs, synthesized with non-toxic ingredients can be a promising candidate for aseptic and therapeutic use.

Supplementary Information The online version contains supplementary material available at https://doi.org/10.1007/s00339-022-05568-z.

Acknowledgements We would like to thank Dr. Banu Taktak Karaca and Biruni University for valuable contributions including Bradford assay, Zeta-potential measurements. Additionally, our sincere gratitude to NANOSILVER Kimya Sanayii Ticaret A.Ş. (Chemical Commerce & Industry Co.) for financial support, Dr. Yonca Alkan Göksü for FT-IR measurements and Selçuk University (ILTEK) for TEM images.

Author contributions MS conceptualized the research, conducted the all the experiments, analyzed the experiment data regarding to characterization of nanoparticles and drafted the manuscript. BB helped both the experiments and preparing the manuscript. SM measured particle size of the samples. ST supervised and provided the necessary materials for nanoparticle synthesis. All authors read and approved the final manuscript.

Data availability The data that support the findings of this study are available from the corresponding author, M.S., upon reasonable request.

Declarations

Conflict of interest The authors declare that they have no competing interests.

References

1. C. N. R. Rao, A. Müller, ve A. K. Cheetham, *The chemistry of nanomaterials: synthesis, properties and applications, 2 Volumes*. 2004. Erişim: 22 Şubat 2022. [Çevrimiçi]. Erişim adresi: https://ui.adsabs.harvard.edu/abs/2004cnsp.book.....R
2. P.M. Mendes, Cellular nanotechnology: making biological interfaces smarter. Chem. Soc. Rev. **42**(24), 9207–9218 (2013). https://doi.org/10.1039/C3CS60198F
3. T.M. Tolaymat, A.M. El Badawy, A. Genaidy, K.G. Scheckel, T.P. Luxton, M. Suidan, An evidence-based environmental perspective of manufactured silver nanoparticle in syntheses and applications: a systematic review and critical appraisal of peer-reviewed scientific papers. Sci. Total Environ. **408**(5), 999–1006 (2010). https://doi.org/10.1016/j.scitotenv.2009.11.003
4. D.M. Eby, N.M. Schaeublin, K.E. Farrington, S.M. Hussain, G.R. Johnson, Lysozyme catalyzes the formation of antimicrobial silver nanoparticles. ACS Nano **3**(4), 984–994 (2009). https://doi.org/10.1021/nn900079e
5. D.M. Mitrano, E. Rimmele, A. Wichser, R. Erni, M. Height, B. Nowack, Presence of nanoparticles in wash water from conventional silver and nano-silver textiles. ACS Nano **8**(7), 7208–7219 (2014). https://doi.org/10.1021/nn502228w
6. K. Jadhav, Phytosynthesis of silver nanoparticles: characterization, biocompatibility studies, and anticancer activity. ACS Biomater. Sci. Eng. **4**(3), 892–899 (2018). https://doi.org/10.1021/acsbiomaterials.7b00707
7. S.P. Deshmukh, S.M. Patil, S.B. Mullani, S.D. Delekar, Silver nanoparticles as an effective disinfectant: a review. Mater. Sci. Eng. C **97**, 954–965 (2019). https://doi.org/10.1016/j.msec.2018.12.102
8. T. Maneerung, S. Tokura, R. Rujiravanit, Impregnation of silver nanoparticles into bacterial cellulose for antimicrobial wound dressing. Carbohydr. Polym. **72**(1), 43–51 (2008). https://doi.org/10.1016/j.carbpol.2007.07.025
9. P. Prasher, Emerging trends in clinical implications of bio-conjugated silver nanoparticles in drug delivery. Colloid Interface Sci. Commun. **35**, 100244 (2020). https://doi.org/10.1016/j.colcom.2020.100244
10. M. Sivera, Silver nanoparticles modified by gelatin with extraordinary pH stability and long-term antibacterial activity. PLoS One **9**(8), e103675 (2014). https://doi.org/10.1371/journal.pone.0103675
11. H. He, In situ green synthesis and characterization of sericin-silver nanoparticle composite with effective antibacterial activity and good biocompatibility. Mater. Sci. Eng. C **80**, 509–516 (2017). https://doi.org/10.1016/j.msec.2017.06.015
12. H. Huang, X. Yang, Synthesis of polysaccharide-stabilized gold and silver nanoparticles: a green method. Carbohydr. Res. **339**(15), 2627–2631 (2004). https://doi.org/10.1016/j.carres.2004.08.005
13. A. de Lima, P.S. da Silva, A. Spinelli, Chitosan-stabilized silver nanoparticles for voltammetric detection of nitrocompounds. Sens. Actuators B Chem. **196**, 39–45 (2014). https://doi.org/10.1016/j.snb.2014.02.005
14. M. Darroudi, M.B. Ahmad, A.H. Abdullah, N.A. Ibrahim, Green synthesis and characterization of gelatin-based and sugar-reduced silver nanoparticles. Int. J. Nanomed. **6**, 569–574 (2011). https://doi.org/10.2147/IJN.S16867
15. N.M. Zain, A.G.F. Stapley, G. Shama, Green synthesis of silver and copper nanoparticles using ascorbic acid and chitosan for antimicrobial applications. Carbohydr. Polym. **112**, 195–202 (2014). https://doi.org/10.1016/j.carbpol.2014.05.081
16. S. Mohan, Completely green synthesis of dextrose reduced silver nanoparticles, its antimicrobial and sensing properties. Carbohydr. Polym. **106**, 469–474 (2014). https://doi.org/10.1016/j.carbpol.2014.01.008
17. L.K.H. Rocha, Sericin from *Bombyx mori* cocoons. Part I: extraction and physicochemical-biological characterization for biopharmaceutical applications. Process Biochem. **61**, 163–177 (2017). https://doi.org/10.1016/j.procbio.2017.06.019
18. O. Akturk, A. Tezcaner, H. Bilgili, M.S. Deveci, M.R. Gecit, D. Keskin, Evaluation of sericin/collagen membranes as prospective wound dressing biomaterial. J. Biosci. Bioeng. **112**(3), 279–288 (2011). https://doi.org/10.1016/j.jbiosc.2011.05.014
19. Y. Yin, Z.-Y. Li, Z. Zhong, B. Gates, Y. Xia, S. Venkateswaran, Synthesis and characterization of stable aqueous dispersions of silver nanoparticles through the Tollens process. J. Mater. Chem. **12**(3), 522–527 (2002). https://doi.org/10.1039/B107469E
20. L. Kvítek, R. Prucek, A. Panáček, R. Novotný, J. Hrbáč, R. Zbořil, The influence of complexing agent concentration on particle size in the process of SERS active silver colloid synthesis. J. Mater. Chem. **15**(10), 1099–1105 (2005). https://doi.org/10.1039/B417007E
21. P. Aramwit, S. Kanokpanont, T. Nakpheng, T. Srichana, The effect of sericin from various extraction methods on cell viability and collagen production. Int. J. Mol. Sci. **11**(5), 2200–2211 (2010). https://doi.org/10.3390/ijms11052200
22. H. Oh, J.Y. Lee, M.K. Kim, I.C. Um, K.H. Lee, Refining hot-water extracted silk sericin by ethanol-induced precipitation. Int.

J. Biol. Macromol. **48**(1), 32–37 (2011). https://doi.org/10.1016/j.ijbiomac.2010.09.008
23 H. Teramoto, M. Miyazawa, Molecular orientation behavior of silk sericin film as revealed by ATR infrared spectroscopy. Biomacromol **6**(4), 2049–2057 (2005). https://doi.org/10.1021/bm0500547
24 D.C. CastrillónMartínez, C.L. Zuluaga, A. Restrepo-Osorio, C. Álvarez-López, Characterization of sericin obtained from cocoons and silk yarns. Proced. Eng. **200**, 377–383 (2017). https://doi.org/10.1016/j.proeng.2017.07.053
25 A.-T. Le, Green synthesis of finely-dispersed highly bactericidal silver nanoparticles via modified Tollens technique. Curr. Appl. Phys. **10**(3), 910–916 (2010). https://doi.org/10.1016/j.cap.2009.10.021
26 A. Panáček, Silver colloid nanoparticles: synthesis, characterization, and their antibacterial activity. J. Phys. Chem. B **110**(33), 16248–16253 (2006). https://doi.org/10.1021/jp063826h
27. S. Sangsuk, Preparation of high surface area silver powder via Tollens process under sonication. Mater. Lett. **64**(6), 775–777 (2010). https://doi.org/10.1016/j.matlet.2010.01.013
28. G.A. Martínez-Castañón, N. Niño-Martínez, F. Martínez-Gutierrez, J.R. Martínez-Mendoza, F. Ruiz, Synthesis and antibacterial activity of silver nanoparticles with different sizes. J. Nanoparticle Res. **10**(8), 1343–1348 (2008). https://doi.org/10.1007/s11051-008-9428-6
29. M. Darroudi, M.B. Ahmad, A.K. Zak, R. Zamiri, M. Hakimi, Fabrication and Characterization of gelatin stabilized silver nanoparticles under UV-light. Int. J. Mol. Sci. **12**(9), 9 (2011). https://doi.org/10.3390/ijms12096346
30 Y.M. Mohan, K.M. Raju, K. Sambasivudu, S. Singh, B. Sreedhar, Preparation of acacia-stabilized silver nanoparticles: a green approach. J. Appl. Polym. Sci. **106**(5), 3375–3381 (2007). https://doi.org/10.1002/app.26979
31. M. Chen, Y.-G. Feng, X. Wang, T.-C. Li, J.-Y. Zhang, D.-J. Qian, Silver nanoparticles capped by oleylamine: formation, growth, and self-organization. Langmuir **23**(10), 5296–5304 (2007). https://doi.org/10.1021/la700553d
32. D. Philip, Green synthesis of gold and silver nanoparticles using Hibiscus rosa sinensis. Phys. E Low-Dimens. Syst. Nanostruct. **42**(5), 1417–1424 (2010). https://doi.org/10.1016/j.physe.2009.11.081
33 S. Shankar, L. Jaiswal, R.S.L. Aparna, R.G.S.V. Prasad, Synthesis, characterization, in vitro biocompatibility, and antimicrobial activity of gold, silver and gold silver alloy nanoparticles prepared from Lansium domesticum fruit peel extract. Mater. Lett. **137**, 75–78 (2014). https://doi.org/10.1016/j.matlet.2014.08.122
34 E.J. Guidelli, A.P. Ramos, M.E.D. Zaniquelli, O. Baffa, Green synthesis of colloidal silver nanoparticles using natural rubber latex extracted from *Hevea brasiliensis*. Spectrochim. Acta. A. Mol. Biomol. Spectrosc. **82**(1), 140–145 (2011). https://doi.org/10.1016/j.saa.2011.07.024
35 K. Jyoti, M. Baunthiyal, A. Singh, Characterization of silver nanoparticles synthesized using *Urtica dioica* Linn. leaves and their synergistic effects with antibiotics. J. Radiat. Res. Appl. Sci. **9**(3), 217–227 (2016). https://doi.org/10.1016/j.jrras.2015.10.002
36 J. Neunzehn, F. Draude, U. Golla-Schindler, H.F. Arlinghaus, H.-P. Wiesmann, Detection of protein coatings on nanoparticles surfaces by ToF-SIMS and advanced electron microscopy. Surf. Interface Anal. **45**(9), 1340–1346 (2013). https://doi.org/10.1002/sia.5287
37. J.F.A. de Oliveira, M.B. Cardoso, Partial aggregation of silver nanoparticles induced by capping and reducing agents competition. Langmuir **30**(17), 4879–4886 (2014). https://doi.org/10.1021/la403635c
38 T. Klar, M. Perner, S. Grosse, G. von Plessen, W. Spirkl, J. Feldmann, Surface-plasmon resonances in single metallic nanoparticles. Phys. Rev. Lett. **80**(19), 4249–4252 (1998). https://doi.org/10.1103/PhysRevLett.80.4249
39 A.M. El Badawy, T.P. Luxton, R.G. Silva, K.G. Scheckel, M.T. Suidan, T.M. Tolaymat, Impact of environmental conditions (pH, ionic strength, and electrolyte type) on the surface charge and aggregation of silver nanoparticles suspensions. Environ. Sci. Technol. **44**(4), 1260–1266 (2010). https://doi.org/10.1021/es902240k
40 W. Liu, Q. Zhou, J. Liu, J. Fu, S. Liu, G. Jiang, Environmental and biological influences on the stability of silver nanoparticles. Chin. Sci. Bull. **56**, 2009–2015 (2011). https://doi.org/10.1007/s11434-010-4332-8
41 I. Fernando, Y. Zhou, Impact of pH on the stability, dissolution and aggregation kinetics of silver nanoparticles. Chemosphere **216**, 297–305 (2019). https://doi.org/10.1016/j.chemosphere.2018.10.122
42 C. Levard, E.M. Hotze, G.V. Lowry, G.E. Brown, Environmental transformations of silver nanoparticles: impact on stability and toxicity. Environ. Sci. Technol. **46**(13), 6900–6914 (2012). https://doi.org/10.1021/es2037405
43 G.K. Vertelov, Y.A. Krutyakov, O.V. Efremenkova, A.Y. Olenin, G.V. Lisichkin, A versatile synthesis of highly bactericidal Myramistin® stabilized silver nanoparticles. Nanotechnology **19**(35), 355707 (2008). https://doi.org/10.1088/0957-4484/19/35/355707
44 F. Ahsan, T.M. Ansari, S. Usmani, P. Bagga, An insight on silk protein sericin: from processing to biomedical application. Drug Res. **68**(6), 317–327 (2018). https://doi.org/10.1055/s-0043-121464
45 S.V. Sokolov, K. Tschulik, C. Batchelor-McAuley, K. Jurkschat, R.G. Compton, Reversible or not? Distinguishing agglomeration and aggregation at the nanoscale. Anal. Chem. **87**(19), 10033–10039 (2015). https://doi.org/10.1021/acs.analchem.5b02639
46 S. Ashraf, Protein-mediated synthesis, pH-induced reversible agglomeration, toxicity and cellular interaction of silver nanoparticles. Colloids Surf. B Biointerfaces **102**, 511–518 (2013). https://doi.org/10.1016/j.colsurfb.2012.09.032
47. I. Kim, B.-T. Lee, H.-A. Kim, K.-W. Kim, S.D. Kim, Y.-S. Hwang, Citrate coated silver nanoparticles change heavy metal toxicities and bioaccumulation of *Daphnia magna*. Chemosphere **143**, 99–105 (2016). https://doi.org/10.1016/j.chemosphere.2015.06.046
48 A.J. Kora, R. Manjusha, J. Arunachalam, Superior bactericidal activity of SDS capped silver nanoparticles: synthesis and characterization. Mater. Sci. Eng. C **29**(7), 2104–2109 (2009). https://doi.org/10.1016/j.msec.2009.04.010
49. J. Hedberg, M. Lundin, T. Lowe, E. Blomberg, S. Wold, I.O. Wallinder, Interactions between surfactants and silver nanoparticles of varying charge. J. Colloid Interface Sci. **369**(1), 193–201 (2012). https://doi.org/10.1016/j.jcis.2011.12.004
50 X. Li, J.J. Lenhart, H.W. Walker, Dissolution-accompanied aggregation kinetics of silver nanoparticles. Langmuir ACS J. Surf. Colloids **26**(22), 16690–16698 (2010). https://doi.org/10.1021/la101768n
51. L. Kvítek, Effect of surfactants and polymers on stability and antibacterial activity of silver nanoparticles (NPs). J. Phys. Chem. C **112**(15), 5825–5834 (2008). https://doi.org/10.1021/jp711616v